

Quantum Critical Point and Entanglement in a Matrix Product Ground State

Amit Tribedi and Indrani Bose

May 26, 2019

Department of Physics

Bose Institute

93/1, Acharya Prafulla Chandra Road

Kolkata - 700 009, India

Abstract

In this paper, we study the entanglement properties of a spin-1 model the exact ground state of which is given by a Matrix Product state. The model exhibits a critical point transition at a parameter value $a = 0$. The longitudinal and transverse correlation lengths are known to diverge as $a \rightarrow 0$. We use three different entanglement measures $S(i)$ (the one-site von Neumann entropy), $S(i, j)$ (the two-body entanglement) and $G(2, n)$ (the generalized global entanglement) to determine the entanglement content of the MP ground state as the parameter a is varied. The entanglement length is found to diverge in the vicinity of the quantum critical point $a = 0$. The first derivative of the entanglement measure $E (= S(i), S(i, j), G(2, n))$ w.r.t. the parameter a also diverges. However, at the QCP itself the entanglement E becomes zero. We further show that multipartite correlations are involved in the QPT at $a = 0$.

I. INTRODUCTION

Quantum phase transitions (QPTs) occur at temperature $T = 0$ and are driven solely by quantum fluctuations [1]. A QPT is brought about by tuning a parameter, either external or intrinsic to the Hamiltonian, to a special value termed the transition point. In the case of a second order phase transition, the point is

known as a quantum critical point (QCP). In thermodynamic critical phenomena, the thermal correlation length diverges and the thermodynamic quantities become singular as the critical point is approached. In the quantum case, the correlation length diverges in the vicinity of the QCP and the ground state properties develop non-analytic features. Entanglement is a unique feature of quantum mechanical systems and serves as an indicator of non-local quantum correlations in the system. An issue of considerable interest is whether the quantum correlations, like the usual correlation functions, become long-ranged near the QCP. In a wider perspective, the major goal is to acquire a clear understanding of the role of entanglement in QPTs. QPTs have been extensively studied in spin systems both theoretically and experimentally. In recent years, several theoretical studies have been undertaken to elucidate the relationship between QPTs and entanglement in spin systems [2, 3, 4, 5, 6, 7]. In particular, a number of entanglement measures have been identified which develop special features close to the transition point. One such measure is concurrence which quantifies the entanglement between two spins ($S = \frac{1}{2}$). At a QCP, as illustrated by a class of exactly-solvable spin models ($S = \frac{1}{2}$), the derivative of the ground state concurrence has a logarithmic singularity though the concurrence itself is non-vanishing upto only next-nearest-neighbour-distances between two spins [2, 3]. Discontinuities in the ground state concurrence have been shown to characterize first order QPTs [8, 9, 10]. Later, Wu et al. [5] developed a general theory to show that a first order QPT, associated with a discontinuity in the first derivative of the ground state energy, gives rise to a discontinuity in a bipartite entanglement measure like concurrence and negativity. Similarly, a discontinuity or a divergence in the first derivative of the same measure is the signature of a second order phase transition, distinguished by a discontinuity or a divergence in the second derivative of the ground state energy. Another measure of entanglement, studied in the context of QPTs, is the entropy of entanglement between a block of L adjacent spins in a chain with the rest of the system [4]. At the QCP, the entropy of entanglement diverges logarithmically with the length of the block. There is, however, no direct relations with the long range correlations.

A number of entanglement measures have recently been proposed which are characterized by a diverging length scale, the entanglement length, close to a QCP. The localizable entanglement (LE) between two spins is defined as the maximum average entanglement that can be localized between them by performing local measurements on the rest of the spins [11]. The entanglement length sets the scale over which the LE decays. The two-body entanglement $S(i, j)$ is a measure of the entanglement between two separated spins, at sites i and j , and the rest of the spins [7]. Let $\rho(i, j)$ be the reduced density matrix for the two spins, obtained from the full density matrix by tracing out the spins other than the ones at sites i

and j . The two body entanglement $S(i, j)$ is given by the von Neumann entropy

$$S(i, j) = -\text{Tr } \rho(i, j) \log_2 \rho(i, j) \quad (1)$$

In a translationally invariant system, S depends only on the distance $n = |j - i|$. As pointed out in [7], spins that are entangled with one or both the spins at sites i and j contribute to S . The two-body entanglement $S(i, j)$ is related to the spin correlation functions in the large n limit. Away from the critical point, $S(i, j)$ is found to saturate over a length scale ξ_E as n increases. Near the QCP, one obtains

$$S(i, j) - S(\infty) \sim n^{-1} e^{-\frac{n}{\xi_E}} \quad (2)$$

The entanglement length (EL), ξ_E , is analogous to that in the case of LE. EL diverges with the same critical exponent as the correlation length at the QCP. $S(i, j)$ thus captures the long range correlations associated with a QPT. At the critical point itself, $S(i, j) - S(\infty)$ has a power-law decay, i.e., $S(i, j) - S(\infty) \sim n^{-\frac{1}{2}}$. The results have been established in the case of the $S = \frac{1}{2}$ exactly solvable anisotropic XY model in a transverse magnetic field which belongs to the universality class of the transverse Ising model [7]. In the limit of large n , the first derivative of $S(i, j)$ w.r.t. a Hamiltonian parameter develops a λ -like cusp at the critical point. The universality and a finite-size scaling of the entanglement have also been demonstrated. The one-site von Neumann entropy

$$S(i) = -\text{Tr } \rho(i) \log_2 \rho(i) \quad (3)$$

is also known to be a good indicator of a QPT [3]. It provides a measure of how a single spin at the site i is entangled with the rest of the system. The reduced density matrix $\rho(i)$ is obtained from the full density matrix by tracing out all the spins except the one at the site i . Oliveira et al. [6] have proposed a generalized global entanglement (GGE) measure $G(2, n)$ which quantifies multipartite entanglement (ME). $G(2, n)$ for a translationally symmetric system is given by

$$G(2, n) = \frac{d}{d-1} [1 - \sum_{l,m=1}^{d^2} |[\rho(j, j+n)]_{lm}|^2] \quad (4)$$

where $\rho(j, j+n)$ is the reduced density matrix of dimension d . The factor 2 in $G(2, n)$ indicates that the reduced density matrix is that for a pair of particles. The first derivative of $G(2, n)$ with respect to a parameter λ involves the first derivatives of the elements of the reduced density matrix with respect to λ . A discontinuity in one or more elements of the reduced density matrix provides the signature of a first order QPT [5]. Thus a discontinuity in $G(2, n)$ signals a first order transition. If $G(2, n)$ is continuous but its first order derivative, $\partial_\lambda G(2, n)$, w.r.t. a parameter λ shows a discontinuity or a divergence, the QPT is of second

order. In the case of the XY $S = \frac{1}{2}$ spin chain, the GGE measure shows a diverging EL as the QCP is approached. The EL $\xi_E = \frac{\xi_C}{2}$ where ξ_C is the usual correlation length. Thus, both the length scales diverge with the same critical exponent near the QCP.

The relationship between entanglement and QPTs has mostly been explored for spin- $\frac{1}{2}$ systems. The entanglement properties of the ground states of certain spin-1 Hamiltonians have been studied using different measures [11, 12, 13]. Numerical studies show that the LE has the maximal value for the ground state of the spin-1 Heisenberg antiferromagnet with open boundary conditions (OBC) [13]. In the case of the spin-1 Affleck-Kennedy-Lieb-Tasaki (AKLT) model [14], the result can be proved exactly. A class of spin-1 models, the ϕ -deformed AKLT models, is characterized by an exponentially decaying LE with a finite EL ξ_E . The length ξ_E diverges at the point $\phi = 0$ though the conventional correlation length remains finite [13]. A recent study [15] shows that in the case of spin-1 systems, the use of LE for the detection of QPTs is not feasible. An example is given by the $S = 1$ XXZ Heisenberg antiferromagnet with single-ion anisotropy. The model has a rich phase diagram with six different phases. The LE is found to be always 1 in the entire parameter region and hence is insensitive to QPTs. The ground states of certain spin-1 models have an exact representation in terms of matrix product states (MPS) [16, 17, 18]. The ground state of the spin-1 AKLT model, termed a valence bond solid (VBS) state, is an example of an MPS. The ground state is characterized by short-ranged spin-spin correlations and a hidden topological order known as the string order. The excitation spectrum of the model is further gapped. In the MPS formalism, ground state expectation values like the correlation functions are easy to calculate. This has made it particularly convenient to study phase transitions in spin models with MP states as exact ground states [17]. The transitions identified so far include both first and second order transitions and are brought about by the tuning of the Hamiltonian parameters. The second order transition in the MP state, however, differs from the conventional QPT in one important respect. The spin correlation function close to the transition point has the standard form $A_C e^{-\frac{n}{\xi_C}}$ for large n . The correlation length ξ_C diverges as the transition point is approached. The pre-factor A_C , however, vanishes at the transition point [17]. This is in contrast to the power-law decay of the correlation function at a conventional QCP. Some distinct features of QPTs in MP states have recently been identified [19]. These states appear to provide an ideal playground for exploring novel types of QPTs. In this paper, we consider a spin-1 model, the exact ground state of which is given by an MP state [20]. The model has a rich phase diagram with a number of first order phase transitions and a critical point transition. We study the entanglement properties of the ground state with a view to pinpoint the special features which appear close to the critical point. This

is done by using three different entanglement measures, namely, the single-site, two-body and generalized global entanglement defined earlier.

II. REDUCED DENSITY MATRIX OF MP GROUND STATE

We consider a spin-1 chain Hamiltonian proposed by Klümper et al. [20] which describes a large class of antiferromagnetic (AFM) spin-1 chains with MP states as exact ground states. The Hamiltonian satisfies the symmetries : (i) rotational invariance in the $x - y$ plane, (ii) invariance under $S^z \rightarrow -S^z$ and (iii) translation and parity invariance. The Hamiltonian has the general form

$$H = \sum_{j=1}^L h_{j,j+1} \quad (5)$$

$$h_{j,j+1} = \alpha_0 A_j^2 + \alpha_1 (A_j B_j + B_j A_j) + \alpha_2 B_j^2 + \alpha_3 A_j + \alpha_4 B_j (1 + B_j) +$$

$$+ \alpha_5 ((S_j^z)^2 + (S_{j+1}^z)^2 + C)$$

where L is the number of sites in the chain and periodic boundary conditions (PBC) hold true. The parameters α_j are real and C is a constant. The nearest-neighbour (n.n.) interactions are

$$A_j = S_j^x S_{j+1}^x + S_j^y S_{j+1}^y \quad (6)$$

$$B_j = S_j^z S_{j+1}^z$$

The constant C in Eq. (5) may be adjusted so that the ground state eigenvalue of $h_{j,j+1} = 0$. Hence

$$h_{j,j+1} \geq 0 \Rightarrow H \geq 0 \quad (7)$$

i.e., H has only non-negative eigenvalues. In the AFM case, the z -component of the total spin of the ground state $S_{tot}^z = 0$. Klümper et al. showed that in a certain subspace of the α_j -parameter space, the AFM ground state has the MP form. Let $|0\rangle$ and $|\pm\rangle$ be the eigenstates of S^z with eigenvalues 0, +1 and -1 respectively. Define a 2×2 matrix at each site j by

$$g_j = \begin{pmatrix} |0\rangle & -\sqrt{a} |+\rangle \\ \sqrt{a} |0\rangle & -\sigma |0\rangle \end{pmatrix} \quad (8)$$

with non-vanishing parameters $a, \sigma \neq 0$.

The global AFM state is written as

$$|\psi_0(a, \sigma)\rangle = \text{Tr}(g_1 \otimes g_2 \otimes \dots \otimes g_L) \quad (9)$$

where ‘ \otimes ’ denotes a tensor product. One can easily check that $S_{tot}^z |\psi_0\rangle = 0$, i.e., the state is AFM. One now demands that the state $|\psi_0(a, \sigma)\rangle$ is the exact ground state of the Hamiltonian H with eigenvalues 0. For this, it is sufficient to show that

$$h_{j,j+1}(g_j \otimes g_{j+1}) = 0 \quad (10)$$

Eq. (3) and (10) are satisfied provided the following equalities

$$\begin{aligned} 1) \sigma &= \text{sign}(\alpha_3), & 2) a\alpha_0 &= \alpha_3 - \alpha_1, \\ 3) \alpha_5 &= |\alpha_3| + \alpha_0(1 - a^2), & 4) \alpha_2 &= \alpha_0 a^2 - 2|\alpha| \end{aligned} \quad (11)$$

and inequalities

$$a \neq 0, \alpha_3 \neq 0, \alpha_4 > 0, \alpha_0 > 0 \quad (12)$$

hold true. The state $|\psi_0(a, \sigma)\rangle$ is the ground state of the Hamiltonian (5) with ground state energy zero provided the equalities in (8) are satisfied. The inequalities constrain the other eigenvalues of $h_{j,j+1}$ to be positive. If the inequalities are satisfied, the ground state can be shown to be unique for any chain length L . Also, in the thermodynamic limit $L \rightarrow \infty$, the excitation spectrum has a gap Δ . With equality signs in the inequalities (12), the state $|\psi_0(a, \sigma)\rangle$ is still the ground state but is no longer unique. The spin-1 model has the typical feature of a Haldane-gap (HG) antiferromagnet. In fact, the AKLT model is recovered as a special case with $a = 2, \sigma = 1, \alpha_3 = 3\alpha_0 > 0, \alpha_2 = -2\alpha_0$ and $\alpha_4 = 3\alpha_0$. The state (9) now represents the VBS state.

Using the transfer matrix method [16], the ground state correlation functions can be calculated in a straightforward manner. The results are ($L \rightarrow \infty, r \geq 2$) :

Longitudinal correlation function

$$\langle S_1^z S_r^z \rangle = -\frac{a^2}{(1 - |a|)^2} \left(\frac{1 - |a|}{1 + |a|} \right)^r \quad (13)$$

Transverse correlation function

$$\langle S_1^x S_r^x \rangle = -|a| [\sigma + \text{sign } a] \left(\frac{-\sigma}{1 + |a|} \right)^r \quad (14)$$

The correlations (13) and (14) decay exponentially with the longitudinal and transverse correlation lengths given by

$$\xi_l^{-1} = \ln \left| \frac{1+|a|}{1-|a|} \right|, \quad \xi_t^{-1} = \ln(1+|a|) \quad (15)$$

Furthermore, the string order parameter has a non-zero expectation value in the ground state. One finds that the correlation lengths diverge as $a \rightarrow 0$, where we have a critical transition. At the point $a = 0$, the correlation functions given by Eq. (13) and (14) are zero. At a conventional QCP, the correlation functions have a power-law decay. We will, however, refer to the point as a QCP since the correlation lengths diverge as the point is approached. We consider a to be ≥ 0 and $\sigma = +1$ in Eq. (8). We now focus on the entanglement properties of the MP ground state (Eq. (9)). The one-site reduced density matrix $\rho(i)$ (Eq. (3)) obtained by tracing out all the spins except the i -th spin from the ground state density matrix $\rho = |\psi_0\rangle\langle\psi_0|$, can be calculated using the transfer matrix method [16]. The density matrix, from Eq. (9), is

$$\rho = |\psi_0\rangle\langle\psi_0| = \sum_{\{n_\alpha, m_\alpha\}} g_{n_1 n_2} g_{n_2 n_3} \dots g_{n_L n_1} g_{m_1 m_2}^\dagger g_{m_2 m_3}^\dagger \dots g_{m_L m_1}^\dagger \quad (16)$$

The summation is over all the indices, $n_i, m_i, i = 1, 2, \dots, L$.

We define a 4×4 matrix f (the elements of which are operators) at any lattice site as

$$f_{\mu_1 \mu_2} \Rightarrow f_{(n_1, m_1)(n_2, m_2)} \equiv g_{n_1 n_2} g_{m_1 m_2}^\dagger \quad (17)$$

The convention of the ordering of the multi-indices is $\mu = 1, 2, 3, 4 \leftrightarrow (11), (12), (21), (22)$. Thus, f can be written as

$$f = \begin{pmatrix} |0\rangle\langle 0| & -\sqrt{a}|0\rangle\langle 1| & -\sqrt{a}|1\rangle\langle 0| & a|1\rangle\langle 1| \\ \sqrt{2}|0\rangle\langle -1| & -|0\rangle\langle 0| & -a|1\rangle\langle -1| & \sqrt{a}|1\rangle\langle 0| \\ \sqrt{a}| -1\rangle\langle 0| & -a| -1\rangle\langle 1| & -|0\rangle\langle 0| & \sqrt{a}|0\rangle\langle 1| \\ a| -1\rangle\langle -1| & -\sqrt{a}| -1\rangle\langle 0| & -\sqrt{a}|0\rangle\langle -1| & |0\rangle\langle 0| \end{pmatrix} \quad (18)$$

Also,

$$\rho(i) = Tr_{1\dots L}^i |\psi_0\rangle\langle\psi_0| \quad (19)$$

where the trace is over all the spins except the i -th one. The transfer matrix F at a site m is obtained by taking the trace over f at the same site, i.e.,

$$F_m = \sum_k \langle k | f_m | k \rangle \quad (20)$$

where the states $|k\rangle$ are the states $|0\rangle$, $|\pm 1\rangle$. The transfer matrix F is obtained as

$$F = \begin{pmatrix} 1 & 0 & 0 & a \\ 0 & -1 & 0 & 0 \\ 0 & 0 & -1 & 0 \\ a & 0 & 0 & 1 \end{pmatrix} \quad (21)$$

The eigenvalues are

$$\lambda_1 = 1 + a, \lambda_2 = 1 - a, \lambda_3 = -1, \lambda_4 = -1 \quad (22)$$

The corresponding eigenvectors are

$$\begin{aligned} |e_1\rangle &= \frac{1}{\sqrt{2}} \begin{pmatrix} 1 \\ 0 \\ 0 \\ 1 \end{pmatrix}, & |e_2\rangle &= \frac{1}{\sqrt{2}} \begin{pmatrix} -1 \\ 0 \\ 0 \\ 1 \end{pmatrix} \\ |e_3\rangle &= \begin{pmatrix} 0 \\ 1 \\ 0 \\ 0 \end{pmatrix}, & |e_4\rangle &= \begin{pmatrix} 0 \\ 0 \\ 0 \\ 1 \end{pmatrix} \end{aligned} \quad (23)$$

From Eq. (20),

$$\rho(i) = \frac{\sum_{\alpha=1}^4 \langle e_\alpha | F^{L-1} f | e_\alpha \rangle}{\sum_{\alpha=1}^4 \langle e_\alpha | F^L | e_\alpha \rangle} \quad (24)$$

The factor in the denominator takes care of the condition $\text{Tr } \rho = 1$. On taking the thermodynamic limit $L \rightarrow \infty$, we get

$$\rho(i) = \lambda_1^{-1} \langle e_1 | f | e_1 \rangle \quad (25)$$

In the $|0, \pm 1\rangle$ basis, the reduced density matrix becomes

$$\rho(i) = \begin{pmatrix} \frac{1}{1+a} & 0 & 0 \\ 0 & \frac{a}{2(1+a)} & 0 \\ 0 & 0 & \frac{a}{2(1+a)} \end{pmatrix} \quad (26)$$

The calculation of the two-site reduced density matrix $\rho(i, j)$ follows in the same manner. $\rho(i, j)$ is given by

$$\rho(i, j) = \text{Tr}_{1..L}^{i,j} |\psi_0\rangle \langle \psi_0| \quad (27)$$

where the trace is taken over all the spins except the i -th and j -th ones.

$$\rho(i, j) = \frac{\sum_{\alpha=1}^4 \langle e_\alpha | F^{i-1} f F^{j-i-1} f F^{L-j} | e_\alpha \rangle}{\sum_{\alpha=1}^4 \langle e_\alpha | F^L | e_\alpha \rangle} \quad (28)$$

In the thermodynamic limit $L \rightarrow \infty$, $\rho(i, j)$ reduces to

$$\rho(i, j) = \sum_{\alpha=1}^4 \lambda_{\alpha}^{-2} \left(\frac{\lambda_{\alpha}}{\lambda_1} \right)^{n+1} \langle e_1 | f | e_{\alpha} \rangle \langle e_{\alpha} | f | e_1 \rangle \quad (29)$$

where $n = |j - i|$.

The matrix $\rho(i, j)$ is a 9×9 matrix and defined in the two-spin basis states $|lm\rangle$ with the ordering

$$|lm\rangle \equiv |11\rangle, |10\rangle, |01\rangle, |1-1\rangle, |-11\rangle, |00\rangle, |0-1\rangle, |-10\rangle, |-1-1\rangle \quad (30)$$

The non-zero matrix elements, b_{pq} ($p = 1, \dots, 9$, $q = 1, \dots, 9$), of $\rho(i, j)$ are :

$$\begin{aligned} b_{11} &= b_{99} = \frac{a^2}{4(1+a)^2} - \frac{a^2}{4(1-a^2)} \left(\frac{1-a}{1+a} \right)^n \\ b_{22} &= b_{33} = b_{77} = b_{88} = \frac{a}{2(1+a)^2} \\ b_{44} &= b_{55} = \frac{a^2}{4(1+a)^2} + \frac{a^2}{4(1-a^2)} \left(\frac{1-a}{1+a} \right)^n \\ b_{23} &= b_{32} = b_{46} = b_{64} = b_{56} = b_{65} = b_{78} = b_{87} = \frac{a}{2(1+a)} \left(-\frac{1}{1+a} \right)^n \\ b_{66} &= \frac{1}{(1+a)^2} \end{aligned} \quad (31)$$

It is easy to check that $\rho(i, j)$ has a block-diagonal form.

III. ENTANGLEMENT MEASURES $S(i)$, $S(i, j)$, $G(2, n)$

We now determine the entanglement content of the ground state $|\psi_0\rangle$ (Eq. (9)) of the Hamiltonian (Eq. (5)) using the entanglement measures $S(i)$, $S(i, j)$, and $G(2, n)$. The calculations are carried out for different values of the parameter a in Eq. (8). The ultimate aim is to probe the special features, if any, of entanglement in the vicinity of the QCP at $a = 0$. From Eq. (3) and (24), the one-site entanglement

$$S(i) = -\text{Tr} \rho(i) \log_2 \rho(i) = -\sum_i \lambda_i \log_2 \lambda_i = \frac{1}{1+a} [(1+a) \log_2 (1+a) - a \log_2 a + a] \quad (32)$$

Figure 1 (top) shows the variation of $S(i)$ w.r.t. a . The one-site entanglement has the maximum possible value $\log_2 3$. This is attained at the AKLT point $a = 2$. The VBS state is in this case the exact ground state. In the VBS state, each spin-1 can be considered as a symmetric combination of two spin- $\frac{1}{2}$'s [14]. In the VBS state, each spin- $\frac{1}{2}$ forms a spin singlet with a neighbouring spin- $\frac{1}{2}$. $S(i)$ has the value zero at the QCP $a = 0$. Figure 1 (bottom) shows the variation of $\frac{\partial S(i)}{\partial a}$

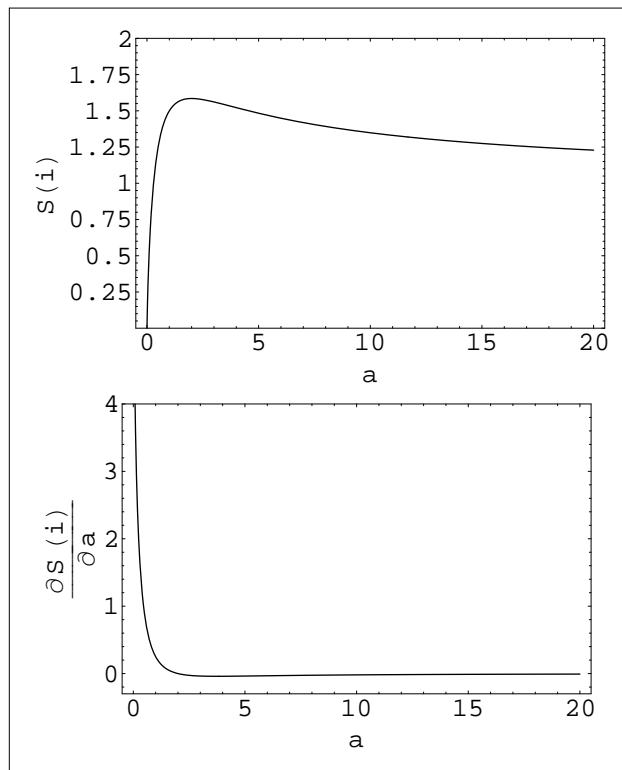


FIG. 1: Plot of $S(i)$ (top) and $\frac{\partial S(i)}{\partial a}$ (bottom) vs. a .

with the parameter a . The derivative diverges as the QCP is approached. This is the expected behaviour at the QCP of a conventional QPT. In the latter case, however, $S(i)$ has the maximum value at the QCP [3].

From Eq. (1) and (31), the two-body entanglement $S(i, j)$ is

$$S(i, j) = - \sum_{i=1}^9 \lambda_i \log_2 \lambda_i \quad (33)$$

The eigenvalues, λ_i 's, of the reduced density matrix are

$$\begin{aligned} \lambda_1 &= \lambda_2 = \frac{a}{2(1+a)^2} - \frac{a}{2(1+a)} \left(-\frac{1}{1+a} \right)^n \\ \lambda_3 &= \lambda_4 = \frac{a}{2(1+a)^2} + \frac{a}{2(1+a)} \left(-\frac{1}{1+a} \right)^n \\ \lambda_5 &= \frac{a^2}{4(1+a)^2} + \frac{a^2}{4(1-a^2)} \left(\frac{1-a}{1+a} \right)^n \\ \lambda_6 &= \lambda_7 = \frac{a^2}{4(1+a)^2} - \frac{a^2}{4(1-a^2)} \left(\frac{1-a}{1+a} \right)^n \\ \lambda_8 &= \frac{1}{2} \left(\frac{a^2}{4(1+a)^2} + \frac{a^2}{4(1-a^2)} \left(\frac{1-a}{1+a} \right)^n + \frac{1}{1+a^2} \right) - \frac{1}{2(1+a)} \\ &\quad \left(\frac{(a^2-4)^2}{16(1+a)^2} + 2a^2 \left(-\frac{1}{1+a} \right)^{2n} + \frac{a^4}{16(1-a)^2} \left(\frac{1-a}{1+a} \right)^{2n} + \frac{a^2(a^2-4)}{8(1-a^2)} \left(\frac{1-a}{1+a} \right)^{2n} \right)^{\frac{1}{2}} \\ \lambda_9 &= \frac{1}{2} \left(\frac{a^2}{4(1+a)^2} + \frac{a^2}{4(1-a^2)} \left(\frac{1-a}{1+a} \right)^n + \frac{1}{1+a^2} \right) + \frac{1}{2(1+a)} \\ &\quad \left(\frac{(a^2-4)^2}{16(1+a)^2} + 2a^2 \left(-\frac{1}{1+a} \right)^{2n} + \frac{a^4}{16(1-a)^2} \left(\frac{1-a}{1+a} \right)^{2n} + \frac{a^2(a^2-4)}{8(1-a^2)} \left(\frac{1-a}{1+a} \right)^{2n} \right)^{\frac{1}{2}} \end{aligned} \quad (34)$$

Knowing the reduced density matrix $\rho(i, j)$, the correlation functions $\langle S_i^\alpha S_j^\alpha \rangle$ ($\alpha = x, y, z$) can be calculated in the usual manner. One then recovers the expressions in Eq. (13) and (14) ($r = n + 1$, where $n = |j - i|$). Figure 2 (top) shows the variation of $S(i, j)$ as a function of a for $n = 1000$. Figure 2 (bottom) shows the variation of the derivative $\frac{\partial S(i, j)}{\partial a}$ w.r.t. a for the same value of n . The maximum of $S(i, j)$ is at the AKLT point $a = 2$ and has the value zero at $a = 0$. For large n , the derivative $\frac{\partial S(i, j)}{\partial a}$ diverges near the QCP at $a = 0$. The last feature is characteristic of a conventional QPT.

We next calculate the GGE $G(2, n)$ (Eq. (4)). This is easily done as the matrix elements of the reduced density matrix (Eq. (3)) are known. Figure 3 (top) shows the variation of $G(2, n)$ versus a for $n = 1000$. Figure 3 (bottom) shows the plot of $\frac{\partial G(2, n)}{\partial a}$ against a . Again $G(2, n)$ has the maximum value at the AKLT point and is zero at $a = 0$. The derivative $\frac{\partial G(2, n)}{\partial a}$ diverges as $a \rightarrow 0$, a feature observed in the case of a conventional QPT [6]. In the latter case, however, $G(2, n)$ has the maximum value at the QCP. Figure 4 (top) shows the plots of $S(i)$, $S(i, j)$, and $G(2, n)$ versus a for $n = 1000$. Figure 4 (bottom) shows the plots of the first derivatives of the same quantities w.r.t. a for $n = 1000$. The plots are shown for comparing the different entanglement measures.

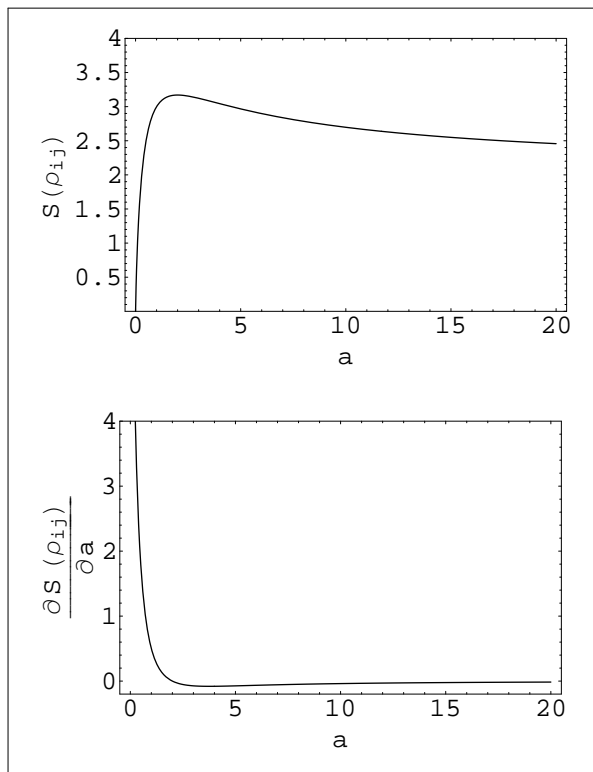


FIG. 2: Plot of $S(i, j)$ (top) and $\frac{\partial S(i, j)}{\partial a}$ (bottom) as a function of a .

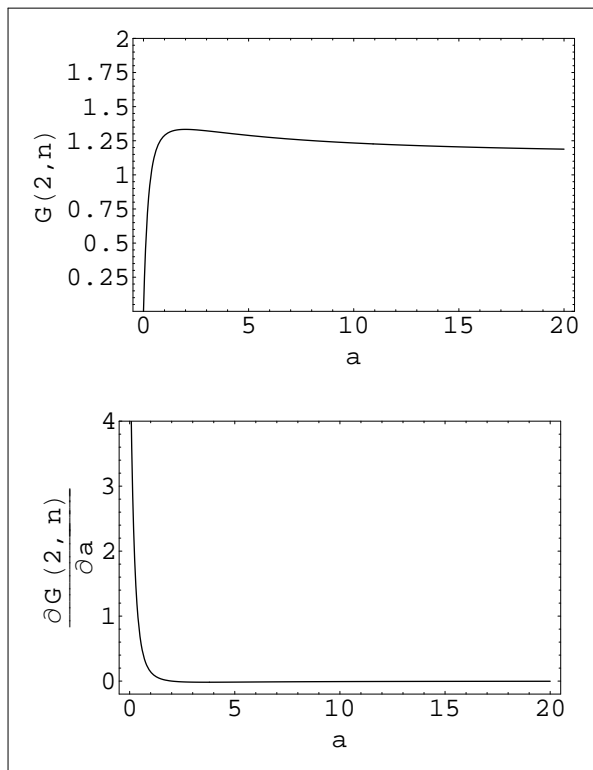


FIG. 3: Plot of $G(2, n)$ (top) and $\frac{\partial G(2, n)}{\partial a}$ (bottom) as a function of a .

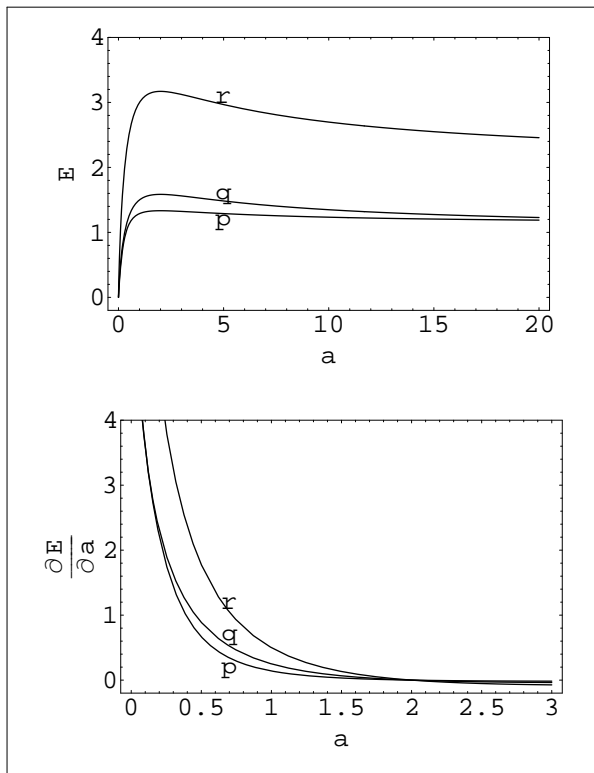


FIG. 4: Plots of $S(i)$ (q), $S(i, j)$ (r), and $G(2, n)$ (p) (top) and the corresponding first derivatives w.r.t. a (bottom) as a function of a . E represents the entanglement measure.

We next determine the EL ξ_E and its variation w.r.t. the parameter a . We consider the entanglement measure $S(i, j)$ for this purpose. Close to the QCP $a = 0$ and in the asymptotic limit of large n , one can write

$$S(n = |j - i|) - S(\infty) \sim A_e e^{-\frac{n}{\xi_E}} \quad (35)$$

The longitudinal and transverse correlation functions, $p_n^z = \langle S_1^z S_{n+1}^z \rangle$ and $p_n^x = \langle S_1^x S_{n+1}^x \rangle$ are given by Eq. (13) and (14) with $r = n + 1$. For $a < 1$, p_n^z decays faster than p_n^x with n . The eigenvalues λ_i 's, $i = 1, \dots, 9$, can be expressed in terms of the correlation functions p_n^z and p_n^x . For large n , the contributions from p_n^z can be ignored. The eigenvalues now reduce to the expressions

$$\begin{aligned} \lambda_1 &= \lambda_2 = \frac{a}{2(1+a)^2} - 4p_n^x \\ \lambda_3 &= \lambda_4 = \frac{a}{2(1+a)^2} + 4p_n^x \\ \lambda_5 &= \frac{a^2}{4(1+a)^2} \\ \lambda_6 &= \lambda_7 = \frac{a^2}{4(1+a)^2} \\ \lambda_8 &= \frac{1}{2} \left(\frac{a^2}{4(1+a)^2} + \frac{1}{1+a^2} \right) - \frac{1}{2} \left(\frac{(a^2-4)^2}{16(1+a)^2} + 2(p_n^x)^2 \right)^{\frac{1}{2}} \\ \lambda_9 &= \frac{1}{2} \left(\frac{a^2}{4(1+a)^2} + \frac{1}{1+a^2} \right) + \frac{1}{2} \left(\frac{(a^2-4)^2}{16(1+a)^2} + 2(p_n^x)^2 \right)^{\frac{1}{2}} \end{aligned} \quad (36)$$

From Eq. (1) and (36), one ultimately arrives at the expressions

$$S(n = |j - i|) - S(\infty) \sim A'_e (p_n^x)^2 \sim A_e e^{-\frac{n}{\xi_E}} \quad (37)$$

The pre-factor $A_e = 0$ at the QCP $a = 0$. The EL ξ_E is given by

$$\xi_E = \frac{\xi_t}{2} = \frac{1}{2 \ln(1 + a)} \quad (38)$$

where ξ_t is the transverse correlation length (Eq. (15)). In the case of the $S = \frac{1}{2}$ anisotropic XY model in a transverse field, an expression similar to that in Eq. (37) is obtained close to the QCP in the limit of large n [7]. The pre-factor in this case, however, does not vanish at the QCP but has a power-law dependence on n . Figure 5 shows the variation of ξ_E w.r.t. a based on the entanglement measure $S(i, j)$. The use of GGE as an entanglement measure yields same expression for the EL.

The total correlations, with both classical and quantum components, between two sites i and j are quantified in terms of the quantum mutual information [21, 22]

$$I_{ij} = S(i) + S(j) - S(i, j) \quad (39)$$

As explained in [21], a comparison of the singular behaviour of $S(i)$ with that of I_{ij} allows one to determine whether two-point ($Q2$) or multipartite (QS) quantum

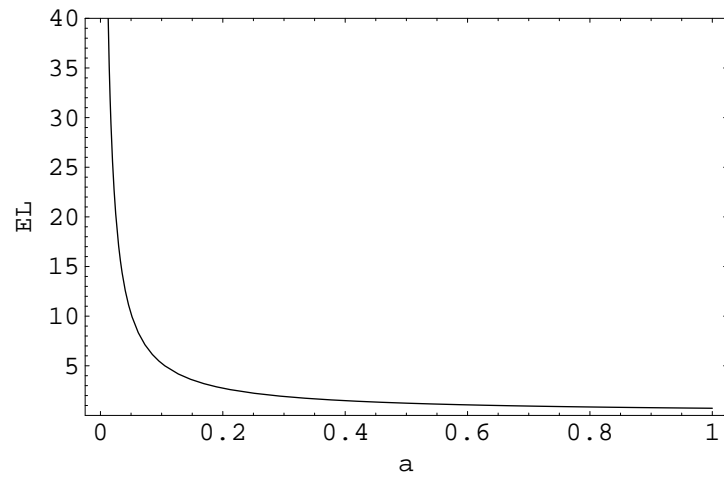


FIG. 5: Plot of EL as a function of a .

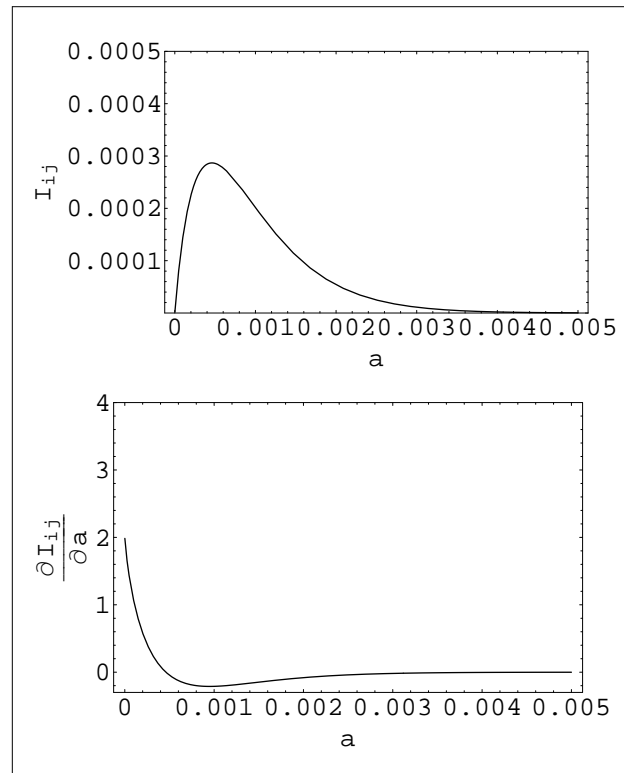


FIG. 6: Plots of I_{ij} (top) and $\frac{\partial I_{ij}}{\partial a}$ (bottom) as a function of a .

correlations are important in a QPT. Figure 6 (top) shows a plot of I_{ij} versus a for $n = 1000$. Figure 6 (bottom) shows the variation of $\frac{\partial I_{ij}}{\partial a}$ versus a for $n = 1000$. The derivative does not diverge as $a \rightarrow 0$, a behaviour distinct from that of $\frac{\partial S(i)}{\partial a}$ close to $a = 0$. The difference in the singular behaviour of quantities associated with $S(i)$ and I_{ij} indicates that multipartite quantum correlations are involved in the QPT. The result is consistent with the feature exhibited by the GGE $G(2, n)$ close to the QCP $a = 0$. $G(2, n)$ provides a measure of multipartite correlations. The associated EL diverges as $a \rightarrow 0$. The first derivative of $G(2, n)$ w.r.t. a also diverges close to the QCP.

IV. DISCUSSIONS

In this paper, we consider a spin-1 model the exact ground state of which is of the MP form over a wide range of parameter values. The model exhibits a novel QPT in that the longitudinal and transverse correlation lengths diverge as the QCP is approached but the correlation functions vanish at the QCP. In a conventional QPT, the correlation functions have a power-law decay at the QCP. We study the entanglement properties of the MP state for different values of the parameter a . The measures used are $S(i)$ (one-site von Neumann entropy), $S(i, j)$ (two-body entanglement) and $G(2, n)$ (GGE). All the entanglement measures have zero value at the QCP so that the ground state is disentangled at that point. As seen from the different plots, figures (1), (2), (3), and (4), the entanglement content, as measured by $E = S(i)$, $S(i, j)$ and $G(2, n)$, has a slow variation w.r.t. a for $a > 2$. At the AKLT point $a = 2$, E reaches its maximum value and as a is reduced further, the magnitude of E falls rapidly to approach zero value at $a = 0$. The EL, however, diverges as $a \rightarrow 0$. Thus, one has the interesting situation that in the vicinity of the QCP at $a = 0$, the entanglement content is reduced as a is decreased but the entanglement is spread over longer distances. The study of conventional QPTs shows that E is maximum at the QCP [3,6,7]. In the present case, the derivative $\frac{\partial E}{\partial a}$ diverges as $a \rightarrow 0$. This feature is similar to what is observed at a conventional QCP. Another analogous feature is that the EL ξ_E is equal to $\frac{\xi_C}{2}$, where ξ_C is the correlation length [6,7]. Figure (4) shows that amongst the three entanglement measures $E = S(i)$, $S(i, j)$ and $G(2, n)$, used in this study to obtain a quantitative estimate of the entanglement content, the measure $S(i, j)$ yields the largest value of entanglement at different values of a . The difference in the singular behaviour of the measures $S(i)$ and the mutual information entropy I_{ij} as $a \rightarrow 0$ indicates that multipartite quantum correlations are involved in the QPT. In summary, the present study highlights the novel aspects of QPT in a spin-1 model, the exact ground state of which is a MP state. Several spin models are known for which the MP states are the exact ground states [17]. Some of these models have interesting

phase diagrams exhibiting both first and second order phase transitions. It will be of interest to extend the present study to other spin models (both $S = \frac{1}{2}$ and 1) in order to identify the universal characteristics of QPTs in MP states.

ACKNOWLEDGMENT

A. T. is supported by the Council of Scientific and Industrial Research, India, under Grant No. 9/15 (306)/ 2004-EMR-I.

References

- [1] S. Sachdev, *Quantum Phase Transitions* (Cambridge University Press, Cambridge, 2000); S. L. Sondhi et al., *Rev. Mod. Phys.* 69, 315 (1997).
- [2] A. Osterloh, L. Amico, G. Falci and R. Fazio, *Nature* 416, 608 (2002).
- [3] T. J. Osborne and M. A. Nielsen, *Phys. Rev. A* 66, 032110 (2002).
- [4] G. Vidal, J. I. Latorre, E. Rico and A. Kitaev, *Phys. Rev. Lett.* 90, 0279011 (2004).
- [5] L. -A. Wu, M. S. Sarandy and D. A. Lidar, *Phys. Rev. Lett* 93, 250404 (2004).
- [6] T. R. de Oliveira, G. Rigolin, M. C. de Oliveira and E. Miranda, *Phys. Rev. Lett.* 97, 170401 (2006).
- [7] H.- D. Chen, *cond-mat/0606126*.
- [8] I. Bose and E. Chattopadhyay, *Phys. Rev. A* 66, 062320 (2002).
- [9] F. C. Alcaraz, A. Saguia and M. S. Sarandy, *Phys. Rev. A* 70, 032333 (2004).
- [10] J. Vidal, R. Mosseri and J. Dukelsky, *Phys. Rev. A* 69, 054101 (2004).
- [11] F. Verstraete, M. Popp and J. I. Cirac, *Phys. Rev. Lett.* 92, 027901 (2004).
- [12] H. Fan, V. Korepin and V. Roychoudhury, *Phys. Rev. Lett.* 93, 227203 (2004).
- [13] F. Verstraete, M. A. Martin-Delgado and J. I. Cirac, *Phys. Rev. Lett.* 92, 087201 (2004).
- [14] I. Affleck, T. Kennedy, E. H. Lieb and H. Tasaki, *Phys. Rev. Lett.* 59, 779 (1987); *Commun. Math. Phys.* 115, 447 (1988).

- [15] L. Campos Venuti and M. Roncaglia, Phys. Rev. Lett. 94, 207207 (2005).
- [16] A. Klümper, A. Schadschneider and J. Zittartz, Z. Phys. B 87, 281-287 (1992).
- [17] A. K. Kolezhuk and H. J. Mikeska, Int. J. Mod. Phys. B 12, 2325 (1998) and references therein.
- [18] M. Fannes, B. Nachtergael and R. F. Werner, Europhys. Lett. 10, 633 (1989); Commun. Math. Phys. 144, 443 (1992).
- [19] M. M. Wolf, G. Ortiz, F. Verstraete and J. I. Cirac, Phys. Rev. Lett. 97, 110403 (2006).
- [20] A. Klümper, A. Schadschneider and J. Zittartz, Europhys. Lett. 24, 293 (1993).
- [21] A. Anfossi, P. Giorda, A. Montorsi and F. Traversa, Phys. Rev. Lett. 95, 056402 (2005).
- [22] A. Anfossi, P. Giorda, A. Montorsi and F. Traversa, cond-mat/0611091.